Energy Equipment and Systems

The required power of the MGT-40 gas turbine starter

Authors

Saadat Zirak [a*]
Hamid Ebrahimi [b]
Ahmad Reza Maissamy [c]

[a] Faculty of Mechanical Engineering Department Semnan University, Semnan, Iran

[b] Aerospace Department Sharif University Of Technology Tehran, Iran

[c] MapnaTurbine Company (TUGA), Karaj, Iran

ABSTRACT

Determination of the starter torque-speed diagram is a major task in the design or selection of a proper gas turbine starter. In this paper, the maximum power of the MGT-40 gas turbine starter was calculated based on the dynamics of the rotor, start-up logic, and compressor map. In a recent research, the pressure ratio was assumed as a linear function of the rotor speed and the required starter power was calculated. In this study, the value is determined from the field data. To evaluate the proposed method, the results of obtained power were compared with that of the turbine performance reports. The comparison resulted in a reasonable engineering approximation.

1. Introduction

The MGT-40 gas turbine is a brand new medium duty product of MAPNA Turbine Co. with 40 MW power at 5100 rpm nominal speed. Its start-up procedure is performed in twelve minutes, of which two minutes is spent for auxiliary system preparation, nine minutes to speed-up the rotor from zero to 60% speed, and the remaining one minute was used to increase the speed beyond 60% and to achieve the nominal no-load speed. The starter is energized by an AC electrical motor and equipped with a hydraulic torque converter. The starter speeds up the turbine rotor up to about 60% and disengaged mechanically due to the centrifugal action of its arms.

Heckel et al. [1] described how to use a computer simulation to size the main starter motors for the single shaft gas turbine.

*Corresponding author: Saadat Zirak
Address: Faculty of Mechanical Engineering Department Semnan University, Semnan, Iran
E-mail address: s_zirak@profs.semnan.ac.ir
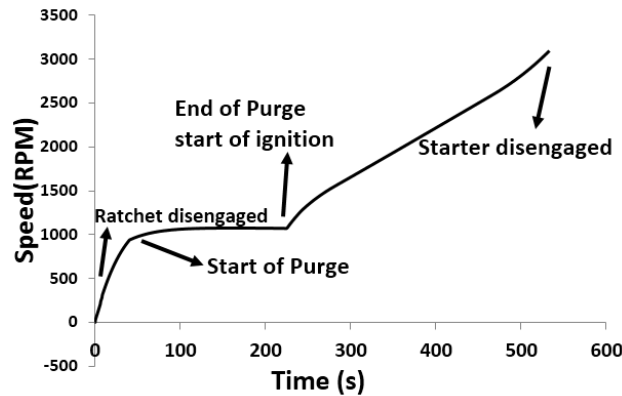
The present research calculated the variation of start-up torque and power with speed, using the dynamics and thermodynamics of turbine rotor together with the compressor map. These results are important in the design and selection of a proper starter system.
Resistant torques against rotor revolution can be categorized as follows:

i)   Total turbine and generator rotors inertia,
ii) Resistance torque of the main flow path,
iii) Frictional torque of the bearings.

The variation of speed versus time is taken from documents and field data and is shown in Fig.1. Start-up begins when the ratchet system is disengaged. Then the purging process takes place, and finally the ignition in the combustion chamber produces an extra power for the starting period. Based on the velocity-time diagram, the rotor angular acceleration is obtained and shown in Fig. 2.

Fig. 1. Start-up speed versus time
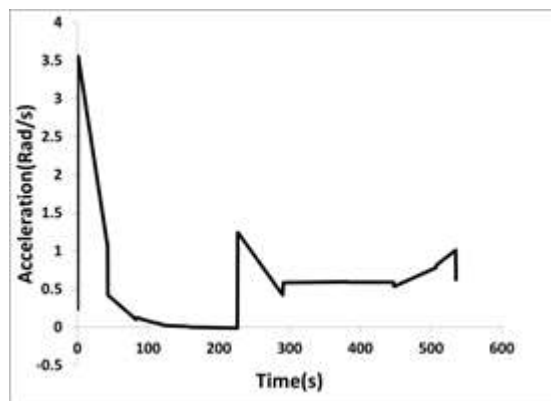
Fig. 2. Start-up rotor angular acceleration versus time

Nomenclatures

M_1	Starter torque
M_2	Main flow torque
M_3	Bearings frictional torque
I	Moment of inertia
m	Rotor mass
G	Gravitational acceleration
μ	Friction coefficient
R	Bearing friction force arm
P	Power
$\dot{m}$	Mass flow rate
C_P	Specific heat
T_t	Stagnation temperature
P_t	Stagnation pressure
T	Bearing frictional torque

Greeks

α	Angular acceleration
ω	Angular velocity
γ	Specific heat ratio
η	Efficiency

Subscripts

c	Compressor
t	Turbine, stagnation
S	Static
K	Dynamic
1	Compressor inlet
2	Compressor outlet
3	Turbine inlet
4	Turbine outlet

2.Rotor Equation of Motion

The accelerating rotor equation of motion is

$$M_1 - M_2 - M_3 = I \times \alpha \qquad (1)$$

where, I refers to the total turbine and generator moment of inertia.

3.Frictional torque of bearings

At the initial revolutions of the rotor, the

bearings resistance is a static type with a frictional coefficient of μ_S , and then decreases to a kinetic type with a μ_k coefficient. The frictional torque is:

$$M_3 = mg\mu R \qquad (2)$$

The results of the bearings friction are as presented in Table (1).

4. Resistance torque of the main flow path

The flow in the main path of the machine produces a resistant torque against the rotor motion as a result of the aerodynamic interaction between the flow and the blades. The resistant torque can be determined using various methods. One of such methods is the application of velocity triangles to calculate the blade forces [2]. Another method involves the use of related developed software which are programmed to evaluate blade forces at off-design points [3, 4]. The method which is the goal of the present work is to use thermodynamic relations to calculate the flow resistant torque as follows [5].

$$P = \dot{m}C_{Pc}(T_{t2} - T_{t1}) \qquad (3)$$
$$+ \dot{m}C_{Pt}(T_{t4} - T_{t3})$$

$$T = \frac{P}{\omega} \qquad (4)$$

$$\eta_t = \frac{C_P(T_{t3} - T_{t4})}{C_P(T_{t3} - T_{tS4})}$$
$$= \frac{\left(\frac{T_{t3}}{T_{t4}} - 1\right)}{\left(\left(\frac{P_{t2}}{P_{t1}}\right)^{\frac{\gamma-1}{\gamma}} - 1\right)} \qquad (5)$$

In two stages of the compressor, fifth and tenth, some part of the flow is bled and finally about 70% of the compressor inlet flow enters the combustion chamber. Estimations show that all compressor stages can be properly analyzed with 83% of the fractional inlet flow.

The major speeds of the start-up period are given in Table 2. The table is divided into two parts, the pre-firing speeds (less than 20%), and the greater post-firing speeds.

4.1.Pre-firing speeds

Pre-firing speeds refer to those rotor revolutions in which the flow is compressed during the compressor stages and then pass through the turbine without any firing in the combustion chamber. Figure 3 shows the thermodynamics T-S diagram of this process.
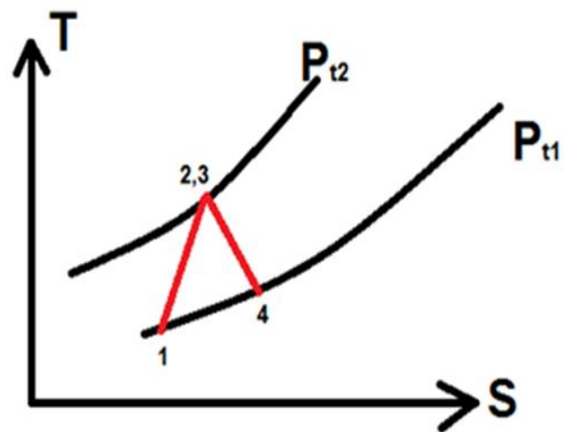
Fig. 3. Thermodynamic cycle of pre-firing process

The flow entered the compressor at state 1, its pressure and temperature increased as a result of the power consumed in the compressor, at the same conditions, enters

Table 1. Bearings of frictional torque parameters

$m\ (kg)$	$R\ (m)$	μ_S	μ_k	$T_S(N.m)$	$T_K(N.m)$
38550	0.14	0.15	0.005	7941.685	264.723

Table 2. Major start-up process speeds

3.87%	5	8.2	18				
200 rpm	258	423.12	928.8				
20%	25	30	35	40	50	55	60
1032 rpm	1290	1548	1806	2064	2580	2838	3096

into the turbine section (state 3), and leaves the turbine at an enthalpy less than that of state 4. During the turbine section, power is generated which is obviously less than the consumed compressor power, but helps the rotor revolution. With a given inlet temperature, the compressor and turbine power is determined with known efficiencies and pressure ratios. The fact that the generated turbine power is less than that of the compressor consumed power indicates that the gas turbine needs to input power in pre-firing speeds which it receives from the starter.

4.2.Post-firing speeds

During the post-firing process (Fig. 4), the combustion chamber is ignited and the inlet temperature of the turbine section is increased to values more than the compressor outlet temperature [6]. It causes more power to be generated in the turbine section and finally the need for starter power vanishes. It happens at 60% revolution, during which the gas turbine is in the so called "self-sustain mode".
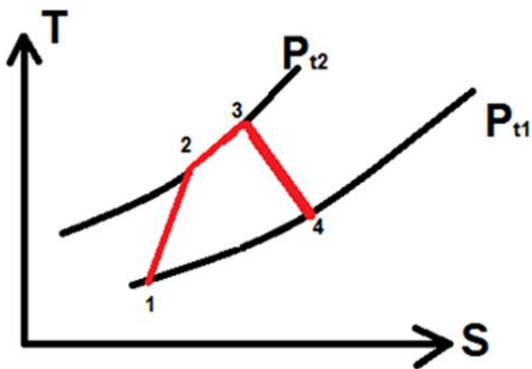
5.Pressure ratio and efficiency

The compressor inlet and outlet temperatures were obtained from documents. Therefore, the compressor power was directly calculated from relation (3) without ascertaining the compressor efficiency. To determine the compressor mass flowrate, the IGV-closed compressor map was used as shown in Fig. 5. The map was obtained from a related 1-D compressor aerodynamics analysis [7, 8].

Pressure ratio was obtained from documents and its variation with speed is shown in Figure 6, for speeds from zero to 60%. Therefore, using map results, the mass flowrate was obtained for various speeds, as shown in Fig.7. In a recent and similar research, due to lack of field data, the pressure ratio was assumed to be a linear function of the rotor revolution [9], but the results were not too different with those of the present real case.
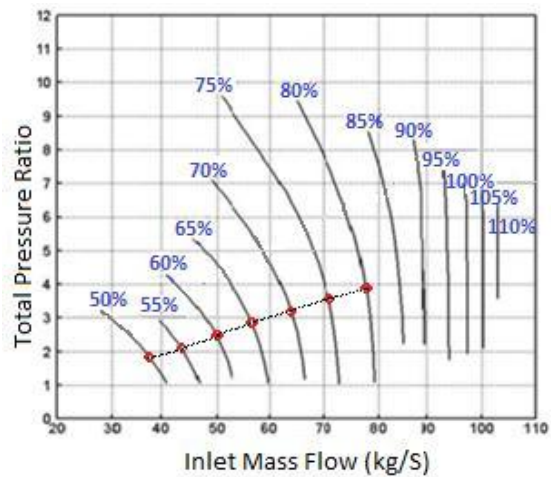

Fig. 4. Post-firing thermodynamic cycle
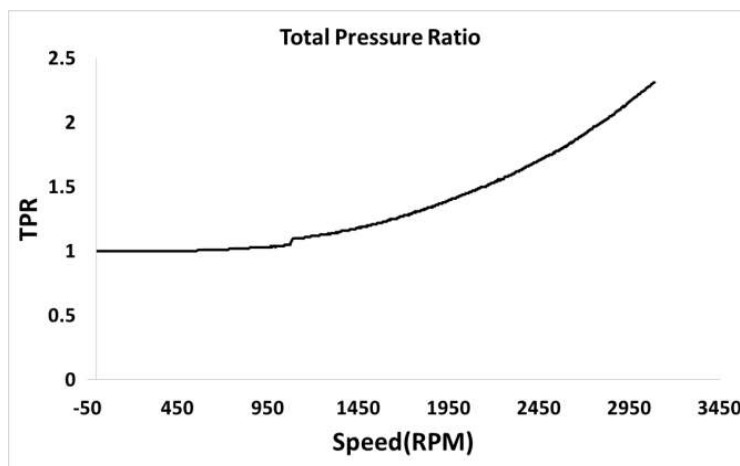

Fig. 5. IGV-closed compressor map

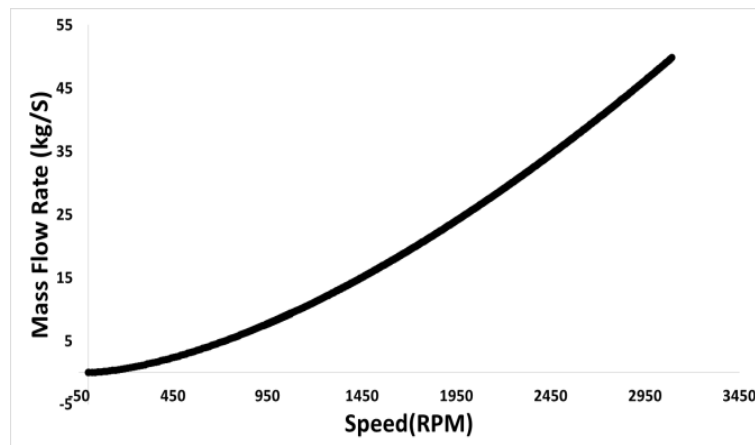**Fig. 6.** Variations of compressor pressure ratio with speed

Fig. 7. Variations of compressor mass flow rate with speed

As mentioned previously, the turbine inlet temperature is the same as the compressor outlet temperature in the pre-firing period, and then becomes greater during post-firing as a result of the combustion process. The turbine temperature can be calculated, so as to achieve a self-sustaining condition at 60% rotor speed.

6.Results

The obtained result of the torque-speed is shown in Fig.8. Similar to other gas turbine systems, the torque value is too large in the initial revolutions of the rotor.

The results of power versus speed were compared with the known power of the AC starter motor in Fig.9. Results of the present method show a maximum power of 300 kW, which is obviously less than the motor power. It is noted that the method considers only the rotor resistant torques mentioned in the previous sections. For a better estimation, other types of resistances should be included in the analysis.

7.Conclusion

In the present work, the required power of the MGT-40 gas turbine starter was obtained through the proposed method. It consists of rotor motion dynamics, flow thermodynamics, field data processing, and a compressor map. The turbine pressure ratio, which was assumed as a linear function of the rotor speed in a previous work, was obtained from the field data. The results of the start-up torque and power was given for various speeds. The obtained power was compared with real values of a similar machine and shows a reasonable engineering approximation.
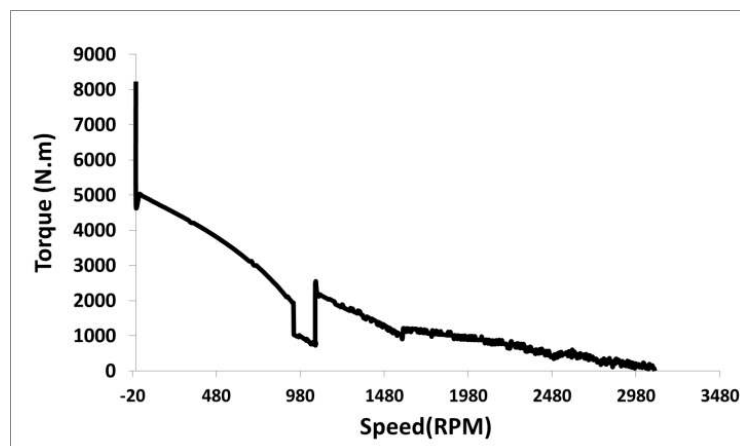
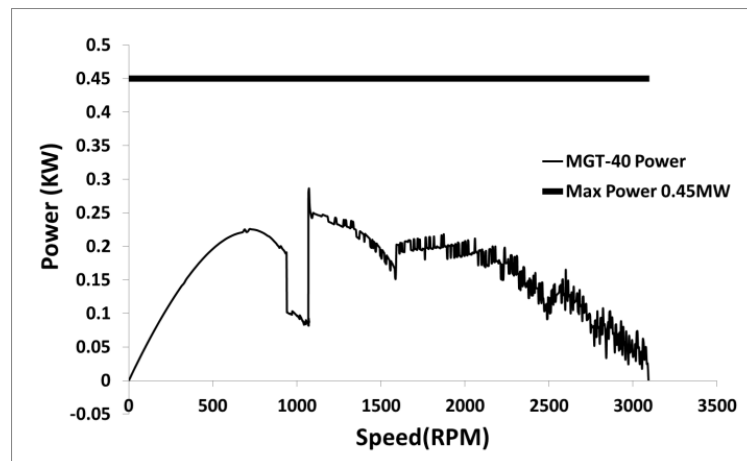## 8.Acknowledgement

Fig. 8. Torque-speed diagram

Fig. 9. Starter power variations with start-up speed

References

[1] Heckel B. G., Davis F. W., Starter Motor Sizing for Gas Turbine (Single Shaft) Driven LNG Strings, Proceedings of the 27th Turbomachinery Symposium, (1998) 7-16.

[2] Hill P., Mechanics and Thermo- dynamics of Propulsion, Second edition (1992).

[3] Mattingly J. , Heiser W., Pratt D., Aircraft Engine Design, Second Edition, (2002).

[4] Mattingly J.,Von Ohain H., Elements of Propulsion, (1989).

[5] Cohen H., Rogers G. F. C., Saravanamuttoo H. I. H., Gas Turbine Theory, Third Edition, (1991).

[6] Cengel Y. A., Boles M. A., Thermodynamics: An Engineering Approach, 7th Edition, Mcgraw-Hill, (2010), ISBN-13: 978-0073529325.

[7] Compressor Meanline Analysis of MGT-40 Gas Turbine, MAPNA Turbine (TUGA), (2015).

[8] Cumpsty N. A., Compressor Aerodynamics, 2th Edition, Krieger Pub Co, (2004), ISBN-13: 978-1575242477.

[9] Ebrahimi H., Zirak S., and Maissamy A. R., Start-Up Torque-Speed Diagram of MGT-40 Gas Turbine, Presented in 4[th]National Gas Turbine Conference (GTC94), Iran University of Science and Technology (IUST), October 6-7 (2015).